Lab on a Chip

PAPER

View Article Online
View Journal

Cite this: DOI: 10.1039/c5lc00582e

Neural probes with multi-drug delivery capability†

Hyogeun Shin,‡[ab] Hyunjoo J. Lee,‡[ac] Uikyu Chae,[ad] Huiyoung Kim,[ae] Jeongyeon Kim,[f] Nakwon Choi,[ab] Jiwan Woo,[f] Yakdol Cho,[f] C. Justin Lee,[fg] Eui-Sung Yoon[ab] and Il-Joo Cho*[ab]

Received 26th May 2015,
Accepted 20th July 2015

DOI: 10.1039/c5lc00582e

www.rsc.org/loc

Multi-functional neural probes are promising platforms to conduct efficient and effective in-depth studies of brain by recording neural signals as well as modulating the signals with various stimuli. Here we present a neural probe with an embedded microfluidic channel (chemtrode) with multi-drug delivery capability suitable for small animal experiments. We integrated a staggered herringbone mixer (SHM) in a 3-inlet microfluidic chip directly into our chemtrode. This chip, which also serves as a compact interface for the chemtrode, allows for efficient delivery of small volumes of multiple or concentration-modulated drugs *via* chaotic mixing. We demonstrated the successful infusion of combinatorial inputs of three chemicals with a low flow rate (170 nl min^{-1}). By sequentially delivering red, green, and blue inks from each inlet and conducting visual inspections at the tip of the chemtrode, we measured a short residence time of 14 s which corresponds to a small swept volume of 66 nl. Finally, we demonstrated the potential of our proposed chemtrode as an enabling tool through extensive *in vivo* mice experiments. Through simultaneous infusions of a chemical (pilocarpine or tetrodotoxin (TTX) at inlet 1), a buffer solution (saline at inlet 2), and 4′,6-diamidino-2-phenylindole (DAPI at inlet 3) locally into a mouse brain, we not only modulated the neural activities by varying the concentration of the chemical but also locally stained the cells at our target region (CA1 in hippocampus). More specifically, infusion of pilocarpine with a higher concentration resulted in an increase in neural activities while infusion of TTX with a higher concentration resulted in a distinctive reduction. For each chemical, we acquired multiple sets of data using only one mouse through a single implantation of the chemtrode. Our proposed chemtrode offers 1) multiplexed delivery of three drugs through a compact packaging with a small swept volume and 2) simultaneous recording to monitor near real-time effects on neural signals, which allows for more versatile *in vivo* experiments with a minimum number of animals to be sacrificed.

Introduction

Multi-functional neural probes[1,2] are promising implantable neuroscience tools for small animals that enable in-depth studies of the brain, such as investigation of functional connectivities and brain disorders. By applying various stimulation modalities (*e.g.* electrical, optical,[3–8] and chemical[9–16]) and simultaneously recording neural signals in a single platform, multi-functional neural probes provide an effective and efficient means to observe the effect of stimulation in real time with minimal damage to brain tissue.

Among these multi-functional neural probes, neural probes integrated with microfluidic channels for direct brain infusion (chemtrodes[9–16]) are of great interest because of the continuously increasing need to assess the efficacy of new pharmaceutical drugs and to investigate the roles of various neurotransmitters. Compared to other methods such as systemic (*e.g.* intravenous, topical and oral) administration, direct brain infusion is the most effective method to deliver drugs due to the presence of blood–brain barrier (BBB).[17] Thus, chemtrodes enable not only targeted drug delivery with an accurate estimation of concentration and quantity of drugs applied on targeted neurons, but also allows near real-time monitoring of changes in neural signals during drug delivery.

[a] *Center for BioMicrosystems, Brain Science Institute, Korea Institute of Science and Technology (KIST), Seoul, Korea. E-mail: ijcho@kist.re.kr*
[b] *Department of Biomedical Engineering, Korea University of Science and Technology (UST), Daejeon, Korea*
[c] *School of Electrical Engineering, Korea Advanced Institute of Science and Technology (KAIST), Daejeon, Korea*
[d] *School of Electrical Engineering, Korea University, Seoul, Korea*
[e] *Department of Mechanical System and Design Engineering, Seoul National University of Science and Technology, Seoul, Korea*
[f] *Center for Neuroscience, Brain Science Institute, Korea Institute of Science and Technology (KIST), Seoul, Korea*
[g] *Department of Neuroscience, Korea University of Science and Technology (UST), Daejeon, Korea*

† Electronic supplementary information (ESI) available. See DOI: 10.1039/celc00582e

‡ These authors contributed equally.

However, currently available implantable chemtrodes are limited to the delivery of a single drug at each implant unless an additional system, such as an external manifold, is used.[9–16] More specifically, once implanted, neither concentrations nor types of drugs can be altered. The only method to deliver more than one drug at a single implant without an additional platform is to load multiple drugs of fixed amounts in a tube at a desired sequence. The drugs are either separated by a small volume of air or placed in direct contact if injection of air is not desired, which inevitably results in undesired mixing at the interfaces of the series of drugs (*i.e.* dispersion). Using this method, a buffer solution can be loaded prior to the drug under test to prevent potential leakage of the drug at the outlet during probe insertion into the brain tissue. However, the serial loading method lacks the multiplexing capability to change the concentration and quantity *in situ* once implanted. If administration of multiple drugs (as separate drugs or a mixture of drugs *in situ*) with fast switching time is possible without the need to remove the inserted neural probe, more effective and efficient animal experiments are possible with a minimum number of animals to be sacrificed. For example, by loading artificial cerebrospinal fluid (aCSF) as a buffer solution, a new pharmaceutical agent, and a dye solution in a multi-drug delivery system, we can examine the pharmacokinetics of the new drug at different concentrations (through mixing the drug with the buffer solution), compare the effects to that of a control, and perform immunostaining, all in a single implantation using one animal. Furthermore, since the dye solution is administrated separately through a different inlet, the quantity of the dye is independently controlled and does not depend on the total amount of the infused drug.

A common method to achieve multi-drug delivery through multiplexing in a single implant is to use an external manifold. A manifold is a mechanical adaptor that consists of multiple inlets and a single outlet placed between an implantable device and a flow control system. By loading different drugs at each inlet, the manifold allows for freedom of combinatorial choices of drugs and freedom to control the quantity and concentration *in situ*. However, this method suffers from a large swept volume when changing drugs because of the relatively large size of the merging reservoir and fluidic channels in the manifold compared with the typical size of microchannels in implantable devices. The swept volume, which is defined as the volume of intended fluids along the flow paths in a microfluidic system, is also an undesired volume during the transitions between multiplexed infusions. Hence, the swept volume determines the switching time of the multiplexed infusion (*i.e.* residence time of drugs between inlets and an outlet to a targeted delivery site). Moreover, the maximum recommended volume for direct brain infusion is relatively small (less than a few microliters for a mouse). Therefore, achieving small swept volumes is critical especially for small animal experiments. Furthermore, simultaneous infusion of multiple drugs *via* the fluidic channels in the manifold typically results in negligible mixing between laminar flow streams. Due to this incomplete mixing, a well-controlled infusion of various concentrations of drugs *in situ* still remains a challenge.

To overcome these problems, miniaturized microfluidic chips have been recently proposed for transdermal drug delivery and microdialysis systems.[18,19] However, no chemtrode with multi-drug delivery capability has been demonstrated for *in vivo* small animal experiments due to the difficulty of achieving a compact packaging. Here we implemented a staggered herringbone mixer (SHM)[20] in a 3-inlet microfluidic chip as a fluidic interface and integrated it into our silicon chemtrode in a compact package (Fig. 1). The presented multi-drug delivery system offers three advantages compared with other existing systems: 1) small swept volume, 2) ability to control the concentration *in situ*, and 3) compact packaging suitable for small animal experiments. We verified the functionality of our chemtrode with multi-drug delivery capability through fluidic characterization using color dyes and extensive *in vivo* mice experiments. Specifically, using our chemtrode with a 3-inlet SHM, we demonstrated the successful modulation of neural activities at different concentrations of two different drugs (pilocarpine and tetrodotoxin (TTX)) and staining of cell nuclei near the injection site, all performed during a single implantation for each drug.

Materials and methods

Fabrication of chemtrode

The silicon-based chemtrode with the embedded microfluidic channels (Fig. 1) was fabricated based on four major steps: 1) etching the cavities and creating a glass cover to form the embedded microfluidic channels in the silicon substrate, 2) patterning of a microelectrode array on top, 3) patterning an inlet and an outlet to provide an interface to the microfluidic channels, and 4) releasing the structure from the backside to create the final shape. The most important aspect of this chemtrode fabrication is the creation of the embedded microfluidic channel; the thin cover is formed by bonding a glass wafer on top of the cavities followed by glass reflow. To improve the process yield during this step, multiple narrow cavities are first created to prevent the glass from completely filling the cavities (see the cross-section of the chemtrode shank in Fig. 2). These sealed channels are then connected in parallel through the inlet and the outlet. The details of the design and fabrication of the chemtrode were previously reported.[11]

Design, fabrication, and packaging of 3-inlet SHM

To achieve multi-drug delivery with our chemtrode, we designed and fabricated a SHM in a 3-inlet polydimethylsiloxane (PDMS) microfluidic chip (Fig. 2). Three inlet channels, connected to three 300 μm-wide, 10 μm-tall cylindrical reservoirs, were twisted to form a serpentine structure, 10 μm in width and 10 μm in height with a total length of 3.3 mm. We designed the serpentine structure with four turns so that the

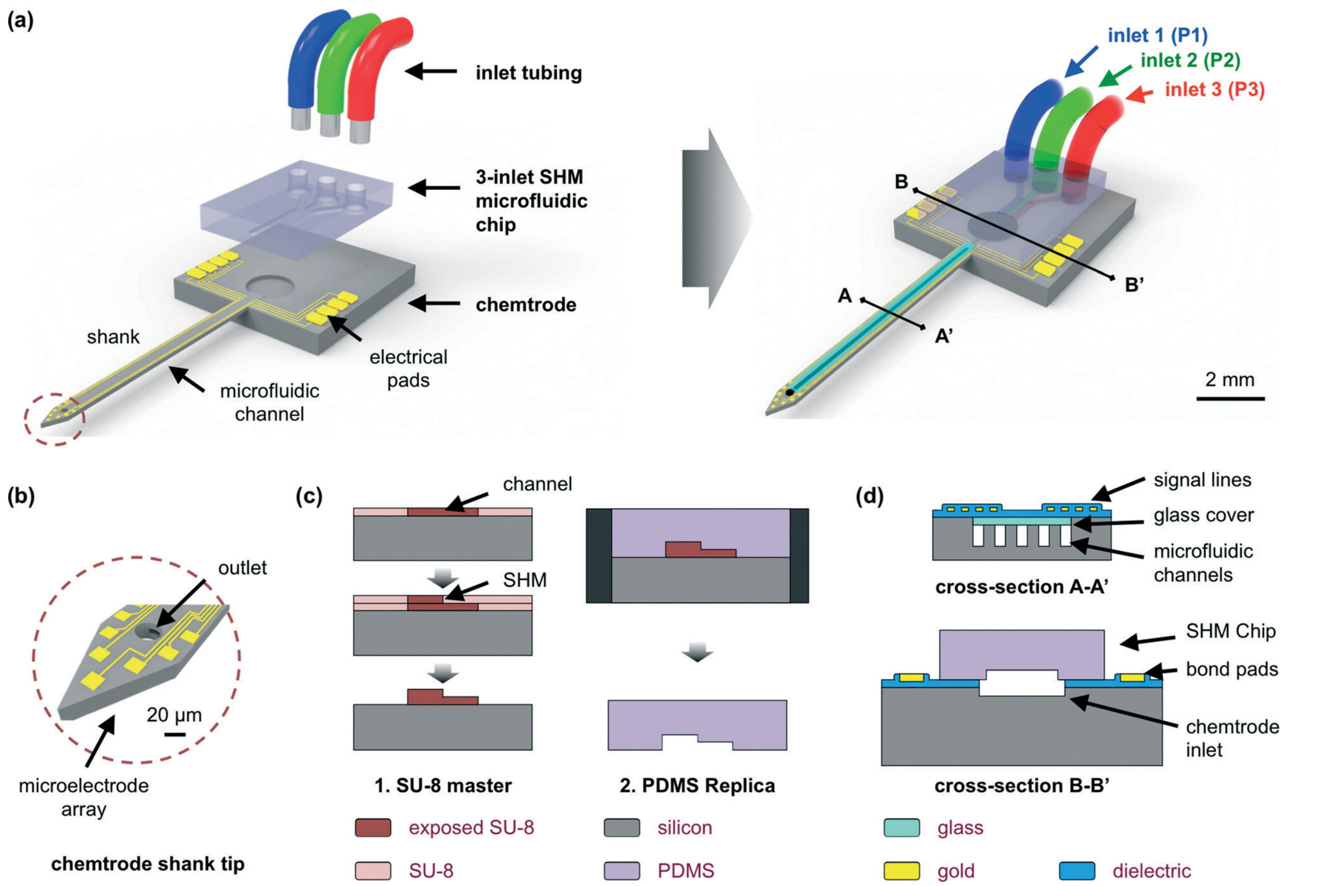

Fig. 1 (a) Conceptual diagram of each component (tubing, 3-inlet SHM chip, and chemtrode) of the proposed neural probe system for multi-drug delivery before and after assembly. (b) Close-in conceptual diagram of the chemtrode shank tip showing the integrated microelectrode array and the outlet. (c) Fabrication process of the SHM chip using the two-layer SU-8 process and the standard PDMS molding process. (d) Cross-section of the chemtrode shank (A-A′) and the probe body (B-B′) showing that the outlet of the SHM chip is aligned to the inlet of the chemtrode.

hydraulic resistance of each inlet channel (R_i) was approximately half the hydraulic resistance of the silicon-glass microchannels in the chemtrode ($R_{chemtrode}$). The ratio of R_i and $R_{chemtrode}$ is an important design parameter to prevent undesired backflows to inlets and to control the mixing ratios precisely with differential input pressures (see the ESI,† Fig. S1). Thus, in our design, the dimensions of the SHM microchannel were minimized. The estimated hydraulic resistances at different pathways in our system show that $R_{chemtrode}$ and R_i were designed to be in the same orders of magnitude (see the ESI,† Fig. S2).

These inlets were merged into a wider microchannel (60 μm in width) with a total length of 7.3 mm. Sixteen half cycles of a staggered herringbone pattern, which was composed of six 15 μm-wide chevron-shaped ridges with a center-to-center spacing of 60 μm, were placed in the PDMS microchannel. The height of the ridge (6 μm) was determined by the optimal ratio of the height of the ridge to that of the microchannel (~0.375) in order to achieve a faster mixing.[21] The microchannel with the SHM was then connected directly to the inlet of the chemtrode. The chemtrode consisted of a 1 mm-wide, 40 μm-tall cylindrical inlet and multiple 9 μm-wide, 7.5 μm-tall, and 9.15 mm-long rectangular microfluidic channels connected in parallel (Fig. 1, inset). The estimated resistance $R_{chemtrode}$ was 21.6 mPa s μm^{-3} for water.

This microfluidic chip, which was also used as the fluidic interface for the chemtrode, was fabricated through a standard fabrication process of PDMS using a SU-8 master. First, the SU-8 master was fabricated on a 4 inch silicon wafer using standard photolithography with two masks. The 3-inlet microfluidic channel was first patterned on a 10 μm-thick SU-8 (SU-8 3010; MicroChem Corp.) layer and then the herringbone ridges were patterned on a 6 μm-thick SU-8 layer (SU-8 3010; MicroChem Corp.) additionally spun on the first layer. Here we used relatively thin SU-8 layers to maximize R_i. The two SU-8 layers were simultaneously developed to produce the patterned microstructures.

After the microfabrication and dicing, the SU-8 master was placed on the bottom of a custom-designed duralumin mold (5 mm × 5 mm × 2 mm). By pouring PDMS (Sylgard 184; Dow Corning) with the curing agent at a mass ratio of 10 : 1 onto this metal mold, degassing in a desiccator, and curing at 85 °C for 2 hr, the SHM pattern on the SU-8 master was transferred to a PDMS replica. The three inlet holes were punctured using a customized punch (inner diameter (ID): 0.3 mm, outer diameter (OD): 0.7 mm). Finally, the

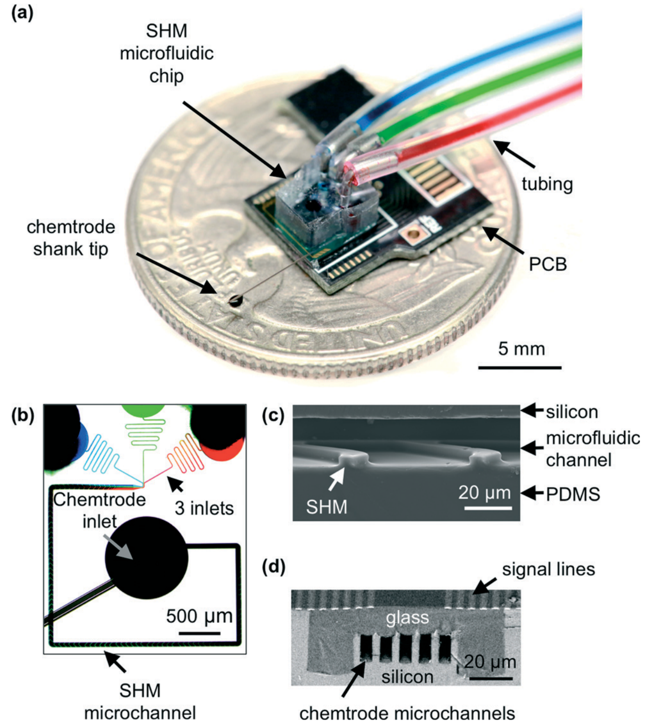

Fig. 2 (a) Optical image of our packaged multi-drug delivery system, showing the 3-inlet SHM chip bonded to our chemtrode. Blue, green, and red dyes loaded at the inputs are mixed in the SHM chip and delivered to the outlet placed at the tip of the chemtrode. (b) Optical image of top view of our 3-inlet SHM chip showing the clear mixing of three dyes. (c) SEM image of the herringbone structure in the PDMS microfluidic chip (upside down). (d) SEM image of the cross-section of the chemtrode shank showing multiple microfluidic channels and signal lines.

micropatterned PDMS replica was manually aligned and bonded to a body portion of the chemtrode by plasma treatment (100 W for 40 s at 50 mTorr; Covance-MP; Femto Science). In addition, to provide electrical connections between the chemtrode and a digital acquisition system (Digital Lynx 4SX; Neuralynx), the chemtrode was glued on a custom-designed printed circuit board (PCB) and electric pads were connected through wire-bonding using gold wires (Fig. 2).

Flow characterization of 3-inlet SHM

We chose a pressure-driven over a displacement-driven delivery method (*e.g.* using a syringe pump) because of the faster response time.[22] Three mass flow controllers (MFC; cDAQ-9171; National Instruments) were connected to an air tank to provide the desired input pressure at each inlet. Multiplexed delivery of multiple drugs was achieved by independently controlling the input voltage of each MFC (see the ESI,† Table S1). A 23 gauge needle was used as an adaptor between Tygon medical tubing (ID: 0.05 cm, OD: 0.15 cm; S-54-HL) and the PDMS microfluidic chip bonded to the chemtrode.

Using our pressure-driven drug delivery system, we first characterized the flow rate. Then, to evaluate the mixer performance, the mixing index (M) was computed for two 2-inlet microfluidic chips with and without SHM (Fig. 3(a)). The mixing index, which is an indicator of the homogeneity of composition in a mixture, is defined in eqn (1) as the variance of the normalized fluorescence intensity,[23]

$$M = \sqrt{\frac{1}{n}\sum_{i=0}^{n}\left(I_n - \langle I \rangle\right)^2} \qquad (1)$$

where n is the number of pixels across the microchannel at a point of interest, I_n is the normalized fluorescence intensity of the nth pixel, and $\langle I \rangle$ is the mean normalized fluorescence intensity of all the pixels. A mixing index of 0.5 indicates no mixing while a mixing index of 0 represents complete mixing. After applying a fixed pressure (100, 150, and 200 kPa) at two inlets, the fluorescence micrographs at 9 different fluidic path lengths for each microchannel were acquired using an inverted microscope (Axio Observer A1; Zeiss) and a complementary metal oxide semiconductor (CMOS) camera (optiMOS™ sCMOS camera; QImaging). Then, the mixing indices (n: 80 pixels) were computed from the acquired images at every 1 mm along the PDMS microchannels. In addition, to evaluate the mixer performance, we characterized the residence time by injecting red, blue, and green inks at each inlet and recording the color changes at the outlet located on the shank tip of the chemtrode immersed in water.

In vivo experimental procedure

One of the main advantages of our chemtrode is the ability to change the concentration of drugs *in situ*. Thus, to demonstrate the functionality, we performed two sets of *in vivo* mice experiments using two different chemicals: pilocarpine and TTX. While pilocarpine, which is often used to develop animal models for epilepsy, is known to increase the firing rate of neural spike signals and to eventually cause epilepsy, TTX is a neurotoxin which inhibits neural firings. By mixing pilocarpine or TTX with a saline solution through our SHM integrated into the chemtrode, we injected different concentrations of these two chemicals and recorded the changes in the firing rate of the neural signals from microelectrodes near the outlet of our chemtrode. At the end of each *in vivo* experiment, we injected 4′,6-diamidino-2-phenylindole (DAPI) through the third inlet to stain the target region and thus to confirm the successful brain infusion using our chemtrode.

All mice experiments were approved by the Korea Institute of Science and Technology (KIST, Seoul, Korea) and performed in accordance with the ethical standards stated in the Animal Care and Use Guidelines of KIST. Adult male mice (C57BL/6, age of 8–12 weeks) were anesthetized through intraperitoneal injection of urethane (1 g kg^{-1}) and mounted on a stereotaxic frame (David Kopf Instruments). After incisions of skins from the surfaces of the skull, stereotaxic coordinates were established based on Franklin and Paxinos, 1997.[24] Then, we drilled two holes through the skull for insertion of a stainless steel bone screw to provide an animal

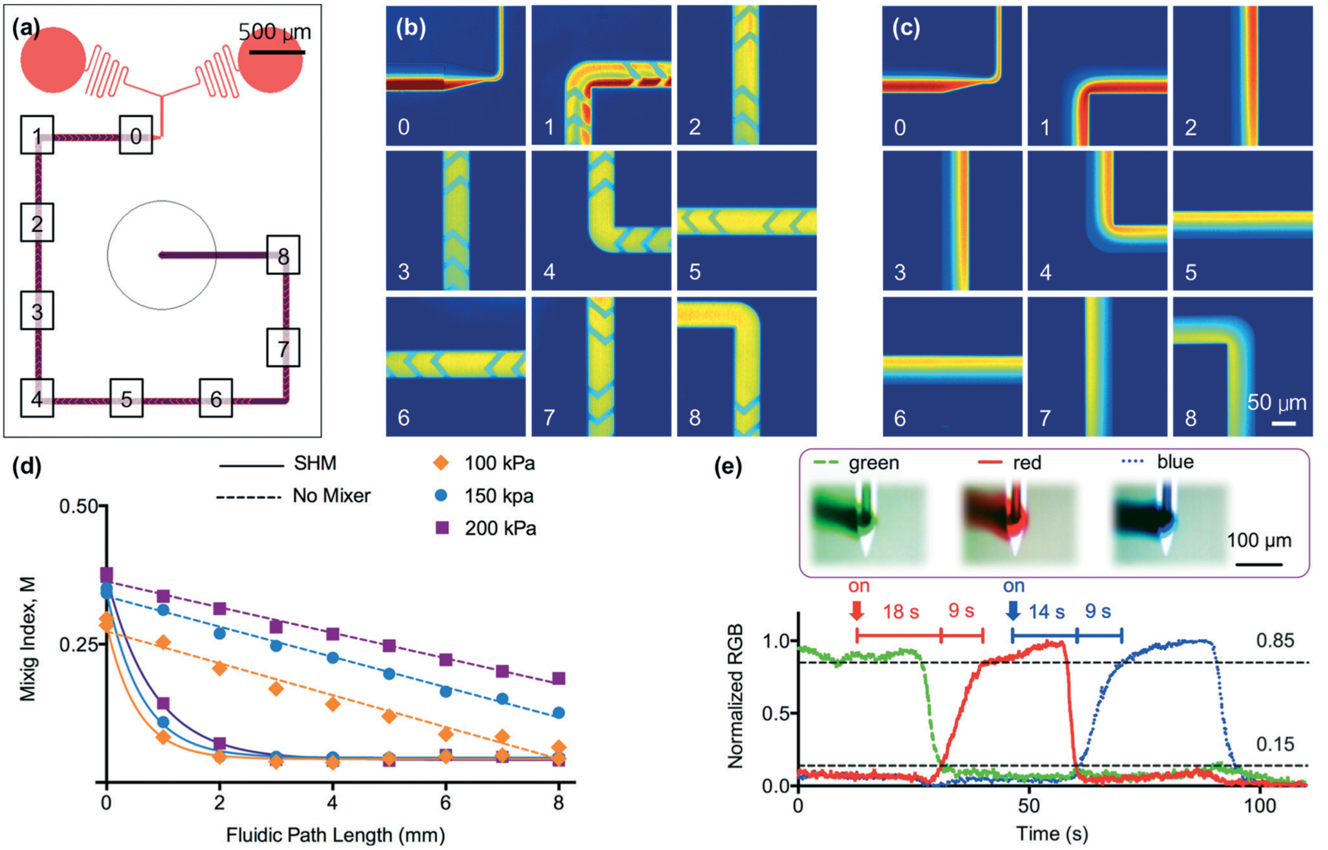

Fig. 3 Characterization of mixer performance. (a) Top view schematic of the 2-inlet SHM chip with boxed numbers indicating the fluidic path length from the inlet. Optical microscope images of the microchannels at every 1 mm of the fluidic path length (b) with SHM and (c) without SHM. (d) Plot of the mixing index over the fluidic path length from the inlet for the microchannels with and without SHM at three different input pressures. (e) Plot of normalized RGB values at the tip of the shank over time. Green, red, and blue dyes were sequentially infused through the packaged chemtrode in water. Inset shows the optical pictures of the tip of the shank when each dye was infused through different inlets.

ground and for insertion of the neural probe at the target region.

We targeted the CA1 region in hippocampus for both sets of experiments (anterior–posterior (AP): −1.6 mm, medial–lateral (ML): 1.7 mm, dorsal–ventral (DV): 1.48 mm from bregma). For each experiment, we loaded a saline solution as a control buffer, a chemical (100 mM pilocarpine hydrochloride and 100 nM TTX; Sigma-Aldrich) as an active drug, and a dye solution (DAPI mounting medium H-1400; Vectashield; Vector Laboratories, Inc.) in our microfluidic chip and applied enough pressure (100 kPa) to load the solutions at each inlet. Prior to inserting the chemtrode into the target brain region, we ensured that the microchannels were prefilled with the saline solution while the drug and dye solutions remained in inlet 2 and 3, respectively. This operation, serving as one of the key advantages of our proposed system, allows for spatiotemporally controlled delivery of small volumes of the active drug to the targeted site; we ensure that the other brain regions near the insertion path of the chemtrode are not exposed to the drug.

After lowering the chemtrode to the target area slowly to minimize the insertion damage, we waited for 30 min for the stabilization of spontaneous neural signals. Then, we injected five different concentrations (0, 25, 50, 75, and 100% of stock concentration of each drug) by adjusting the input pressures for the saline (inlet 1) and the active drug (inlet 2). For each experiment, we injected 125 nl of the solution for 30 s at a flow rate of 250 nl min^{-1} and monitored the changes in the neural signals after the injection for 10 min. After monitoring the neural activities at five different concentrations of each drug, we injected 2 μl of the DAPI solution through inlet 3 to stain the cell nuclei near the injection site.

We used the digital recording system to record the local field potential (LFP) and individual neural spike signals from 16 microelectrodes integrated into our chemtrode at a sampling rate of 32 kHz. Individual neural spikes were obtained by applying a bandpass filter with cutoff frequencies of 300 and 6000 Hz. We performed spike sorting and data analysis on the recorded data for each microelectrode using our custom code implemented in MATLAB (MathWorks).

Results and discussion

SHM-integrated chemtrode

Prior to assessing the performance of the SHM, we first measured the flow rates through our chemtrode integrated with the 3-inlet SHM by applying the same input pressure at inlets 1 and 2 (P_1 and P_2, see Fig. 1). We applied a lower pressure at inlet 3 (P_3: 40 kPa) to prevent backflows during this characterization. By varying P_1 and P_2 from 50 to 200 kPa, we confirmed a linear increase in flow rates ranging from 110 to 660 nl min^{-1} (see the ESI,† Fig. S3). A potential explanation for the slight decrease in flow rate at low input pressure (*e.g.* 50 kPa) is the increased frictional resistance in the microchannels (most likely due to the surface roughness of the silicon-etched microchannels in the chemtrode).[25] These flow rates are suitable for small animal experiments which often involve delivery of small volumes of chemicals (<2 μl) at low flow rates. Given that the sum of the input pressures at 3 inlets (*i.e.* $P_1 + P_2 + P_3$) is constant, the overall flow rates of our system are the same even when we use a different number of inputs (*i.e.* 1, 2, and 3) (see the ESI,† Fig. S1).

We implemented the SHM between multiple inlets and the chemtrode to achieve faster mixing of various solutions through chaotic advection.[20,21] To evaluate the mixing performance, we used two different 2-inlet microfluidic chips with and without the SHM (Fig. 3(a)). For each 2-inlet microfluidic chip, we injected deionized (DI) water and a 10 μM fluorescein solution as a fluorescent tracer *via* microchannels and computed the mixing indices at every 1 mm. As predicted, for the same applied input pressure, we observed complete mixing ($M < 0.1$) after three herringbone half cycles (~approximately 2 mm from the inlets) whereas significantly slow mixing through only lateral diffusion was observed in the microchannel without the mixer (Fig. 3(b)–(d)). These results indicate that despite the relatively small size of our SHM channel compared to other works,[20,21] successful mixing was achieved. Furthermore, these results suggest that the length of the microchannel and thus the swept volume can be further minimized in a next design by utilizing the SHM.

Another important performance metric for a mixer with a multiplexing capability is the swept volume, which is the total volume of a chemical passing in a microfluidic system. Since the goal of our direct brain infusion system is to infuse multiple chemicals at a single implantation, the swept volume, which is an unnecessary yet inevitable volume infused during multiplexing, must be minimized. To estimate the swept volume, we measured the residence time of color inks as model solutions in our 3-inlet microfluidic chip. Note that the residence time is defined as the time required to completely flush out the previously delivered solution.

Green, red, and blue inks were loaded at inlet 1, 2, and 3, respectively, and inlet 1 was driven first. After confirming the successful infusion of the green ink at the chemtrode tip, the red and blue inks were delivered sequentially at 13 and 46 s, respectively, at a flow rate of 170 nl min^{-1} (Fig. 3(e)). If we define that a drop to 15% of normalized color intensity indicates complete wash out of the previous solution, the residence times are estimated to be approximately 18 and 14 s for changing from green to red and red to blue, respectively. These measured values agree well with our estimation for the residence time of ~14 s based on the total internal volume (~40 nl) of the microfluidic chip and the flow rate (170 nl min^{-1}). To deliver the next solution at input concentration to the outlet of our chemtrode, an additional transition time of ~9 s was required. This transition time was attributed to dispersion between two distinct solutions along the fluidic path length from the inlets of the microfluidic chip to the outlet of our chemtrode. This data indicates that infusion of additional 26 nl was required to reach the target region when changing drugs. Nevertheless, the total volume required for the complete input transition (~66 nl) is smaller than typical volumes infused directly in brain (~1 μl).

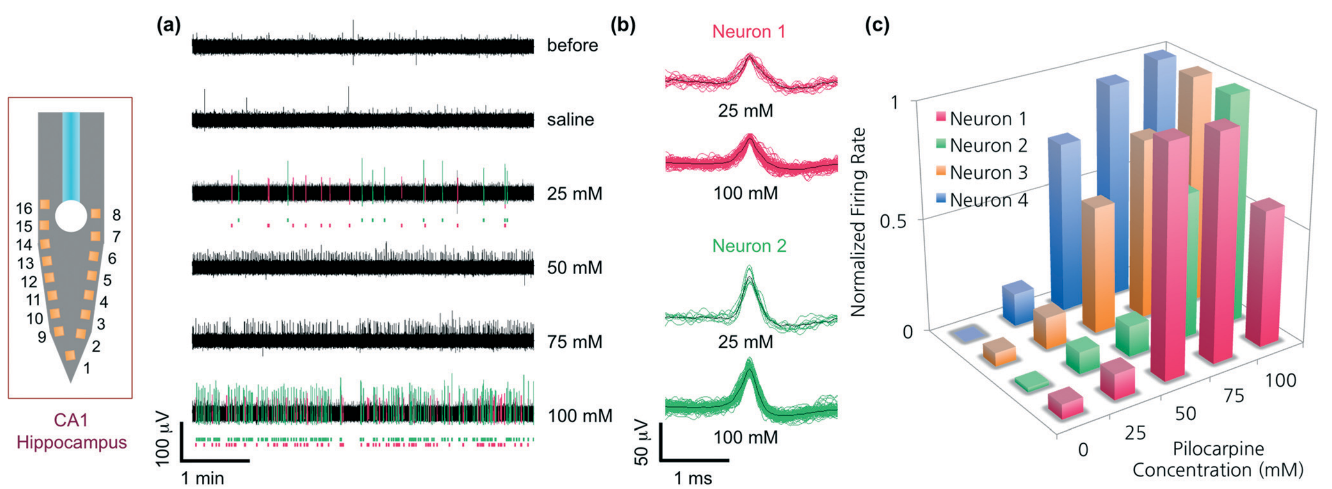

Fig. 4 *In vivo* recording results from direct injection of pilocarpine. The inset on the left shows the spatial distribution of the channels (Ch) and numbering of the microelectrode array. (a) Transient plots of individual neural spikes from Ch 1 over 5 min at different concentrations. 'Before' indicates the state when no solution was infused. Raster plots for 25 and 100 mM are shown below the transient plots. (b) Two sorted neural signals at 25 and 100 mM are shown at a smaller time scale. (c) Normalized firing rates of four sorted neurons at 5 different concentrations of pilocarpine.

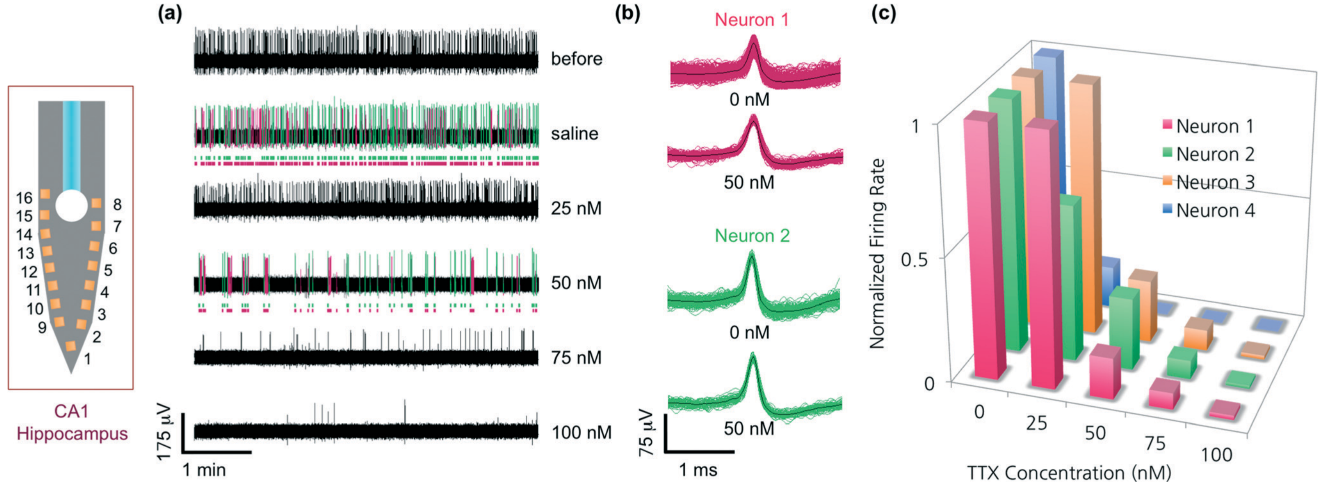

Fig. 5 *In vivo* recording results from direct injection of TTX. The inset on the left shows the spatial distribution of the channels (Ch) and numbering of the microelectrode array. (a) Transient plots of individual neural spikes from Ch 9 over 5 min at different concentrations. 'Before' indicates the state when no solution was infused. Raster plots for 0 and 50 nM are shown. (b) Two sorted neural signals at 0 and 50 nM are shown at a smaller time scale. (c) Normalized firing rates of four sorted neurons at 5 different concentrations of TTX.

In vivo neural modulation through direct brain infusion of various concentrations of drugs

For both *in vivo* mice experiments, spontaneous neural activities were detected on all microelectrodes on the chemtrode as we lowered the shank of the chemtrode towards the CA1 region in hippocampus using the stereotaxic stage. During the direct brain infusion, almost no spontaneous neural activities were detected. One potential explanation for the disappearance of the neural signals is that the infused chemicals resulted in temporal swelling at the target region and neurons near the chemtrode consequently receded from the microelectrode array. After approximately 45 s from the direct brain infusion, neural spike signals from the same neurons re-appeared. This reappearance confirmed through neural sorting indicates that damage due to the infusion was minimal on the neurons under analysis. Considering this temporal disappearance and reappearance of the neural spikes, we recorded the neural signals over a relatively long period of time (10 min) after the completion of the infusion. Since the response time of neurons to the injected drugs appears to be larger than the recovery time of the neural spike activity, the inability to record the neural activity during drug injection is not a major concern in our current system. However, a delivery method that allows simultaneous monitoring of neural activities during drug delivery would be useful.

The last five minutes of the recorded neural spike signals after the infusion of different concentrations of pilocarpine showed a continuous increase in the number of neural spike signals (Fig. 4(a)). As an example, we illustrate the spike signals from two distinct neurons detected on one of the microelectrodes (Ch 1) for two concentrations of pilocarpine (Fig. 4(b)). For the analysis, we examined the firing rates of four neurons from two different neural spike signals detected on two microelectrodes (Ch 1 and Ch 2) (see the ESI,† Fig. S4). As expected[26,27] the number of detected neural signals for all four neurons increased as the concentration of pilocarpine increased (Fig. 4(c)).

An opposite trend of neural modulation was observed for the second *in vivo* experiment (Fig. 5). When infusing various concentrations of TTX, we observed a decrease in the firing rates of the four sorted neural spike signals.[28] Similar to the analysis performed on the previous pilocarpine *in vivo* data, we estimated the firing rates of two neurons detected on two microelectrodes (Ch 9 and Ch 10) at five different concentrations (see the ESI,† Fig. S5). These *in vivo* results illustrate that multi-drug delivery with multiplexing capability was successfully implemented in a microfluidic chip with a size comparable to that of our previous chemtrode system.[11] In addition, since neural probe systems are implanted directly above mouse heads, the size of the total system is critical for long-

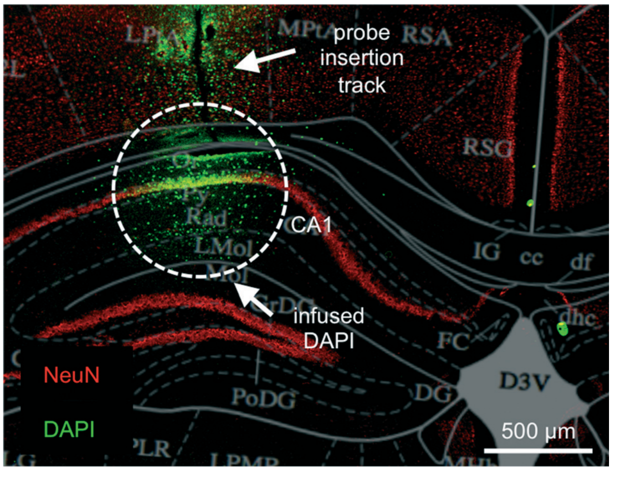

Fig. 6 Confocal fluorescence micrograph of the brain slice with post-staining of neurons using NeuN (shown in red). Successful infusion of DAPI using the chemtrode is shown in green.

term chronic *in vivo* experiments. Thus, our chemtrode with the compact SHM chip is also a promising candidate for chronic applications, which is part of our future work. Furthermore, these *in vivo* results demonstrate that our chemtrode with multi-drug delivery capability would be an effective tool to study the pharmacokinetics of drugs and to investigate the fundamental mechanisms behind brain disorders by modulating neural circuits by delivering neurotransmitters through a single implant.

We also performed immunohistology on the brain of the sacrificed mouse to confirm the infused areas of the DAPI solution near the CA1 region (Fig. 6). A representative confocal fluorescence micrograph of brain slices reveals that we targeted our chemtrode correctly in the CA1 region. In addition, cell nuclei, stained by DAPI *in situ* (dotted region in Fig. 6), clearly indicate the spread of directly infused solutions at the target region. (Note that we post-stained neurons on the brain slice with a neuronal biomarker, NeuN.)

Conclusions

We proposed and presented a chemtrode with multi-drug capability by using a SHM in a 3-inlet microfluidic chip as a microfluidic interface for the chemtrode. Our SHM allows for rapid mixing of drugs in a small microfluidic chip that is integrated into the chemtrode body. In addition, by offering multiplexing capability and controllability of drug concentrations with a low swept volume for direct brain infusion, our chemtrode enables new designs of *in vivo* experiments not only to elucidate the brain circuitry more effectively, but also to reduce the number of required animals to study the pharmacokinetics of drugs by allowing the modulation of doses (*i.e.* concentration) *in situ*.

Acknowledgements

This work was partially supported by KIST Institutional Program (2E25474) and the Original Technology Research Program for Brain Science through the National Research Foundation of Korea (NRF) funded by the Ministry of Education, Science and Technology (2012M3C7A1055410).

References

1 A. Canales, X. Jia, U. P. Froriep, R. A. Koppes, C. M. Tringides, J. Selvidge, C. Lu, C. Hou, L. Wei and Y. Fink, *Nat. Biotechnol.*, 2015, 277–284.
2 B. Rubehn, S. B. Wolff, P. Tovote, A. Lüthi and T. Stieglitz, *Lab Chip*, 2013, **13**, 579–588.
3 A. M. Aravanis, L.-P. Wang, F. Zhang, L. A. Meltzer, M. Z. Mogri, M. B. Schneider and K. Deisseroth, *J. Neural Eng.*, 2007, **4**, S143.
4 H. Cao, L. Gu, S. Mohanty and J. Chiao, *IEEE Trans. Biomed. Eng.*, 2013, **60**, 225–229.
5 I.-J. Cho, H. Won Baac and E. Yoon, 2010.
6 S. Royer, B. V. Zemelman, M. Barbic, A. Losonczy, G. Buzsáki and J. C. Magee, *Eur. J. Neurosci.*, 2010, **31**, 2279–2291.
7 M. Schwaerzle, K. Seidl, U. Schwarz, O. Paul and P. Ruther, 2013.
8 F. Wu, E. Stark, M. Im, I.-J. Cho, E.-S. Yoon, G. Buzsáki, K. D. Wise and E. Yoon, *J. Neural Eng.*, 2013, **10**, 056012.
9 A. Altuna, E. Bellistri, E. Cid, P. Aivar, B. Gal, J. Berganzo, G. Gabriel, A. Guimerà, R. Villa and L. J. Fernández, *Lab Chip*, 2013, **13**, 1422–1430.
10 J. Chen, K. D. Wise, J. F. Hetke and S. Bledsoe, *IEEE Trans. Biomed. Eng.*, 1997, **44**, 760–769.
11 H. J. Lee, Y. Son, J. Kim, C. J. Lee, E.-S. Yoon and I.-J. Cho, *Lab Chip*, 2015, **15**, 1590–1597.
12 A. Pongrácz, Z. Fekete, G. Márton, Z. Bérces, I. Ulbert and P. Fürjes, *Sens. Actuators, B*, 2013, **189**, 97–105.
13 P. Rohatgi, N. B. Langhals, D. R. Kipke and P. G. Patil, *Neurosurg. Focus*, 2009, **27**, E8.
14 K. Seidl, S. Spieth, S. Herwik, J. Steigert, R. Zengerle, O. Paul and P. Ruther, *J. Micromech. Microeng.*, 2010, **20**, 105006.
15 S. Spieth, A. Schumacher, K. Seidl, K. Hiltmann, S. Haeberle, R. McNamara, J. Dalley, S. Edgley, P. Ruther and R. Zengerle, *4th European Conference of the International Federation for Medical and Biological Engineering*, Antwerp, Belgium, 2008.
16 S. Takeuchi, D. Ziegler, Y. Yoshida, K. Mabuchi and T. Suzuki, *Lab Chip*, 2005, **5**, 519–523.
17 H. J. Lee, Y. Son, D. Kim, Y. K. Kim, N. Choi, E.-S. Yoon and I.-J. Cho, *Sens. Actuators, B*, 2015, **209**, 413–422.
18 A. T. Evans, S. Chiravuri and Y. B. Gianchandani, 2010.
19 M. L. Rogers, D. Feuerstein, C. L. Leong, M. Takagaki, X. Niu, R. Graf and M. G. Boutelle, *ACS Chem. Neurosci.*, 2013, **4**, 799–807.
20 A. D. Stroock, S. K. Dertinger, A. Ajdari, I. Mezić, H. A. Stone and G. M. Whitesides, *Science*, 2002, **295**, 647–651.
21 C. A. Cortes-Quiroz, M. Zangeneh and A. Goto, *Microfluid. Nanofluid.*, 2009, **7**, 29–43.
22 K. W. Bong, S. C. Chapin, D. C. Pregibon, D. Baah, T. M. Floyd-Smith and P. S. Doyle, *Lab Chip*, 2011, **11**, 743–747.
23 T. Nguyen, M.-C. Kim, J.-S. Park and N.-E. Lee, *Sens. Actuators, B*, 2008, **132**, 172–181.
24 G. Paxinos and K. B. Franklin, *The mouse brain in stereotaxic coordinates*, Gulf Professional Publishing, 2004.
25 K. V. Sharp, R. J. Adrian, J. G. Santiago and J. I. Molho, *The MEMS Handbook*, ed. Mohamed Gad-El-Hak, CRC Press, Boca Raton, 2002.
26 A. Cymerblit-Sabba and Y. Schiller, *J. Neurosci.*, 2010, **30**, 1619–1630.
27 C.-H. Wang, C. P. Hung, M.-T. Chen, Y.-H. Shih and Y.-Y. Lin, *PLoS One*, 2012, **7**, e39763.
28 G. G. Turrigiano, K. R. Leslie, N. S. Desai, L. C. Rutherford and S. B. Nelson, *Nature*, 1998, **391**, 892–896.

